IMPACT-INDUCED MELTING BY GIANT IMPACT EVENTS. L. Manske[1,2], K. Wünnemann[1,2], M. Nakajima[3] and A.-C. Plesa[4], [1]Museum für Naturkunde, Leibniz Institut for Evoluton and Biodiversity Science, 10115 Berlin, Germany, (lukas.manske@mfn-berlin.de), [2]Institute for Geological Science, Freie Universität Berlin, 12249 Berlin, Germany, [3]Department of Terrestrial Magnetism, Carnegie Institution for Science Washington, DC 20005, USA, [4]German Aerospace Center (DLR), 12489 Berlin, Germany.

Introduction: We revisited the long-standing problem of the generation of melt as a consequence of giant impact events, which may not be accurately addressed by classical scaling-laws [1,2,3]. Giant collisions such as the Moon-forming event on the young Earth or basin-forming impacts are known to have influenced the chemical and thermal evolution of the terrestrial planets [4]. Besides the material that is delivered by such impacts, a significant amount of energy is transferred to the planet resulting in heating up its interior, which may result in the formation of local magma ponds up to global magma oceans. Existing scaling-laws can predict the amount of shock melting [1,2,3] generated by impacts smaller than basin-forming events. On the scale of giant collisions such scaling laws may not be accurate as they do not account for the initial temperature or lithostatic pressure of planets' interior. This may be problematic for younger planets, where the initial temperatures are close to the solidus. To better understand and quantify the mechanism of heat production and melting during large-scale impact events we conducted a series of numerical models and determined the volume of melt production.

Methods: To model hypervelocity collisions we use the iSALE Eulerian shock physics code [5,6] (Version *Dellen*). In iSALE the thermodynamic state (EoS) is calculated by look-up tables derived from ANEOS [eg. 7] for basalt, dunite, and iron representing the planetary crust, mantle and core, respectively.

Melt calculation. To determine the distribution and volume of impact-induced melting we calculate the local (post-impact) final temperature T_f via the peak shock pressure method; first, we determine the complete thermodynamic state, when the material experiences the highest shock pressure P_{peak} (peak shock pressure). In a second step, we recalculate the thermodynamic release path to the final (confining) pressure P_f using ANEOS and assuming relaxation to an equilibrium state via ANEOS for a given depth. This procedure enables to determine the final temperature T_f of the material, which we compare with the solidus and liquidus temperature $T_{S/L} = f(P_f)$ to assess whether the material is (partially) molten or not. The different material specific solidus and liquidus temperatures $f(P_f)$ are based on previous work [8]. To record the materials peak shock pressure P_{peak} and final pressure P_f, we use massless Lagrangian tracers. Each tracer is associated with the mass of material in the cell, where the tracer was initially located in. As tracers also track the movement of the material, this approach allows for taking decompression melting into account. Decompression is a consequence of displacement of material in the course of crater formation resulting in a lower lithostatic pressure of a given mass unit after crater formation than before impact. To measure the influence of decompression melting, we compare the temperature increase caused by the shock $\Delta T = T_f - T_i$ with the change of the solidus or liquidus caused by the variations of lithostatic pressure due to the displacement (cf. Figure 2, left). T_i describes the initial temperature.

Model. For different terrestrial planets we assume individual initial conditions regarding composition and temperature distributions, typical impact velocities, and gravity. For the impactor we also assume a dunitic composition and neglect differentiated bodies at this stage. In case of the Mars we consider the crust consists of basalt while the initial thermal profiles ($T_i = f(P)$) differ from hot to cold setups, representing earlier to more recent stages of the planet's thermal evolution respectively [9]. In all models the projectile radius is resolved by 50 cells (50 CPPR). For very large impacts we account for the curvature of the target.

Results: For each planet model, we systematically vary the impactor diameter L and velocity v_i for different temperature conditions T_i. Reference models without the effects of gravity, material strength, and depth-dependent temperature, but with a planet-like layered target have been calculated, which can be directly compared with classical scaling-laws.

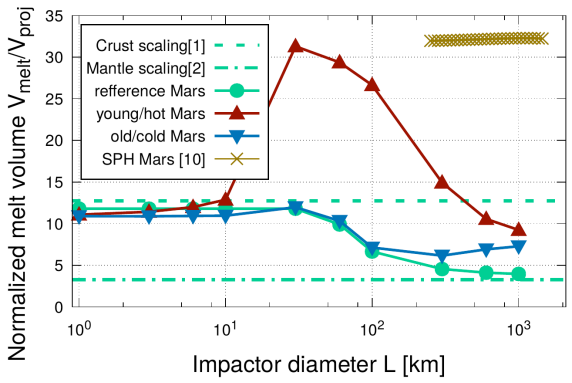

Figure 1. : Normalized melt production assuming Mars-like parameters for different thermal states at 15km/s impactor speed. We show classical scaling laws [1,2] and a direct comparable reference model (green). More realistic models (triangles) are based on different temperature profiles corresponding to different ages after planet formation (red: 40 Myr/ blue: 4500 Myr)[9]. SPH code simulations are presented in ocher [10].

Figure 1 shows that the reference model agrees with the scaling-laws as a function of the impactor diameter L depending on whether crustal or mantle melting dominates. The more realistic models (considering temperature gradient etc., as described in Methods) are approximately in agreement with classic scaling for smaller impacts; however, larger significantly deviate. We find that if the impactor size is in excess of a certain threshold diameter, the shock-induced normalized melt production ($V_{melt}/V_{projectile}$) is more or less significantly increased. This depends on the initial temperature T_i reflecting the evolutionary state of the planet. The increase in melt production results from the fact that for a "warm" planetary interior less shock heating (ΔT_M) is required to induce melting than for a planet, where the temperature difference between T_S (solidus) and T_i as a function of depth is larger. It can be shown that the maximum normalized melt production occurs at an impactor size, where the main melt body is located in a depth where the smallest amount of ΔT_M is required to cause melting (where the temperature profile approaches the solidus). This area is often located close to the bottom of the lithosphere.

For even bigger impactor sizes, SPH code simulations have been added [10] (yellow crosses). Those simulations are based on a temperature profile, where T_i is equal to the solidus T_S. This assumption may hold true for a certain depth range of the young Mars model as well. Using an impactor diameter of 30 km, most of the melt is produced in this depth range, which makes the normalized melt volumes comparable to the SPH model. One can see, that although melt volumes have been derived differently in the iSALE and SPH models, the results are very similar (same level of about $V_{melt}/V_{projectile} = 30$).

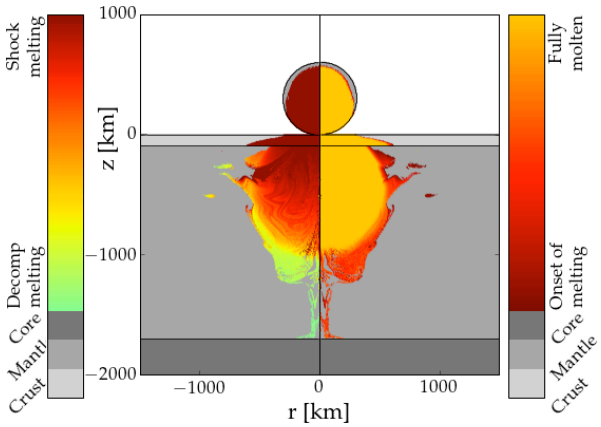

Figure 2.: Melt distribution mapped back to the initial Position. Colors indicate molten material. Left: Influence of decompression melting. Right: Degree of partial melt.

Additionally we find that decompression melting contributes to melt production in an area where the initial temperature profile approaches the solidus. The effect of decompression melting is very sensitive to the chosen initial temperature T_i and solidus (or liquidus) $T_{L/S}$. However, in most cases the decompression melting causes only partial melting to a small degree (cf. Figure 2).

Based on our systematic modeling study we aim at providing a parameterization or a lookup table for the volume of impact-induced melt V_m as a function of impact parameters V_m = f(L, v_i, T_i, P_f) for collision events arbitrary in scale, using SPH and iSALE simulations.

Acknowledgments: We gratefully acknowledge the developers of iSALE, including Gareth Collins, Kai Wünnemann, Dirk Elbeshauesn, Boris Ivanov and Jay Melosh. This work was funded by the Deutsche Forschungsgemeinschaft (SFB-TRR 170, subproject C2 and C4).

References: [1] Abramov O. et al. (2012) Icarus 218, 906-916. [2] Pierazzo et al. (1997) Icarus 127, 408-423, 1997. [3] Bjorkman, M. D. and Holsapple K. A. (1987) Int. J. Impact Eng. 5, 155–163. [4] Marchi S. et al. (2014) Nature 511, 578-582. [5] Collins. G. S. et al. (2004) Meteoritics & Planet. Sci. 39, 217-231.[6] Wünnemann K. et al. (2006) Icarus 180, 514–527. [7] Melosh H. J. (2007) Meteoritics & Planet. Sci. 42, 2079-2098. [8] Ruedas, T. and Breuer, D. (2017) JGR, 122, 1554-1579 [9] Plesa, A.-C. et al. (2016) JGR 121, 2386-2403. [10] Nakajima et al. (2016) AGU, P51A-2118.